Remote Sensing of Environment 170 (2015) 121–132

Contents lists available at ScienceDirect

Remote Sensing of Environment

journal homepage: www.elsevier.com/locate/rse

Regional detection, characterization, and attribution of annual forest change from 1984 to 2012 using Landsat-derived time-series metrics

Txomin Hermosilla [a,*], Michael A. Wulder [b], Joanne C. White [b], Nicholas C. Coops [a], Geordie W. Hobart [b]

[a] Integrated Remote Sensing Studio, Department of Forest Resources Management, University of British Columbia, 2424 Main Mall, Vancouver, British Columbia V6T 1Z4, Canada
[b] Canadian Forest Service (Pacific Forestry Centre), Natural Resources Canada, 506 West Burnside Road, Victoria, British Columbia V8Z 1M5, Canada

ARTICLE INFO

Article history:
Received 24 March 2015
Received in revised form 12 August 2015
Accepted 21 September 2015
Available online 30 September 2015

Keywords:
Change detection
Landsat
Temporal analysis
Image compositing
Object based change

ABSTRACT

The examination of annual, gap-free, surface reflectance, image composites over large areas, made possible by free and open access to Landsat imagery, allows for the capture of both stand replacing and non-stand-replacing forest change. Furthermore, the spatial and temporal information extracted from the time-series data enables the attribution of various forest change types over large areas. In this paper we apply spectral trend analysis of Landsat Thematic Mapper (TM) and Enhanced Thematic Mapper Plus (ETM+) data from 1984 to 2012 to detect, characterize, and attribute forest changes in the province of Saskatchewan, Canada. Change detection is performed using breakpoint analysis of the spectral trends and change events are characterized using a set of metrics derived from an image time series that relate the temporal, spectral, and geometrical properties on an object basis. Change objects are attributed to a change type (i.e., fire, harvesting, road, and non-stand-replacing changes) using a Random Forest classifier. Non-stand-replacing changes are generally low magnitude, punctual, trend anomalies that relate year-on-year ephemeral changes that do not lead to a change in land cover class (i.e., phenology, insects, water stress). The results confirm that land cover changes are detected with high overall accuracy (92.2%), with the majority of changes labeled to the correct occurrence year (91.1%) or within ±1 year (98.7%). Characterization of changes enables accurate attribution both at the object (91.6%) and area levels (98%), with fire and harvesting events the most successfully attributed (commission error < 10%), and roads, the most challenging to attribute correctly (commission error > 13%). Our approach, prototyped over the forested area of Saskatchewan, has enabled a highly automated and systematic depiction of a 30-year history of forest change, providing otherwise unavailable insights on disturbance trends including spatial, temporal, and categorical characteristics. The generation and application of metrics that relate a range of change characteristics allow for depiction of a broad range of change events, types, and conditions.

1. Introduction

The availability of detailed, accurate, and up-to-date land cover and land-cover change information is essential to monitor and manage forest ecosystems (Townshend et al., 2011). Precise knowledge of rates and trends of landscape changes, as well as the responses of these ecosystems to previous disturbance events, enable an improved understanding of how forests will respond to present and future disturbance events (Cole, Bhagwat, & Willis, 2014; Gómez, White, & Wulder, 2011). In Canada forest-dominated ecosystems occupy a large extent, at approximately 60% of the nation's area (Wulder, White, Cranny, et al., 2008a, 2008b). Canadian boreal forest systems remain largely intact (Powers, Coops, Nelson, Wulder, & Drever, 2013), with wildfire predominating in more northern ecosystems, and anthropogenic activities preferentially located in proximity to settled areas and where forest productivity is highest (Andrew, Wulder, & Coops, 2012; Brandt, Flannigan, & Maynard, 2013). On average, from the more than 300 million ha forested and wooded lands of the Canadian boreal zone (Brandt, 2009), approximately 2 million ha are impacted annually by wildfires (Stocks et al., 2002),1 million ha by harvesting activities, and 45,000 ha deforested (Masek et al., 2011). The distinction between harvesting and deforestation must be noted, as harvesting does not result in a land-use change, whereas deforestation implies a long-term or permanent land use change (i.e., forest to agriculture or urban). Stand replacing disturbances can result in both long- or short-term alteration of land cover (Gong & Xu, 2003; Pickell, Gergel, Coops, & Andison, 2014a). Roads, urbanization, or industrial activity within the boreal forest can result in a permanent land-cover modification. In contrast, stand replacing disturbances such as harvesting and fire impose changes in land cover which subsequently returns to a vegetated state (Schroeder, Wulder, Healey, & Moisen, 2011). Non-stand-replacing disturbance events, which are typically more subtle, represent low-magnitude variations in the condition of a given land cover type and do not necessarily involve a cover change (Lehmann, Wallace, Caccetta, Furby, & Zdunic, 2013). These changes can be sporadic

* Corresponding author.
E-mail address: txomin.hermosilla@live.forestry.ubc.ca (T. Hermosilla).

http://dx.doi.org/10.1016/j.rse.2015.09.004
0034-4257/

(e.g., defoliation, diseases), or more cyclical, driven by hydrological and/or weather regimes, such as phenological variations, stressed vegetation, or desiccation processes.

Data from the Landsat series of satellites provide detailed description of the Earth's surface, with temporal and spatial resolutions suitable for monitoring and mapping both natural disturbances and human activity and impact over wide areas (Wulder et al., 2008b). Free and open access to Landsat imagery resulted in maximizing the information content of the archive, at both spatial (i.e., large area) and temporal (i.e., long term) scales (Banskota, Kayastha, Falkowski, & Wulder, 2014; Hansen & Loveland, 2012; Wulder, Masek, Cohen, Loveland, & Woodcock, 2012). Spatially, novel pixel-based compositing approaches have emerged to produce cloud-free, radiometrically consistent image composites that are spatially contiguous using images from multiple Landsat scenes for regional to global land cover monitoring applications (Griffiths, Linden, Der Kuemmerle, & Hostert, 2013; Hansen et al., 2011; Roy et al., 2010; White et al., 2014). Temporally, the richness of the Landsat archive over Canada (White & Wulder, 2013) enables users to detect both stand replacing and non-stand-replacing land cover and condition changes with greater sensitivity and reliability by analyzing spectral trends (Fraser, Olthof, Carrière, Deschamps, & Pouliot, 2012; Huang et al., 2010; Kennedy, Yang, & Cohen, 2010). Besides detecting and dating these land-cover changes, trend analysis of the long-term spectral response can provide a detailed characterization of disturbance events (e.g. magnitude, duration), as well as pre- and post-change condition (Bolton, Coops, & Wulder, 2015; Frazier, Coops, Wulder, & Kennedy, 2014; Hermosilla, Wulder, White, Coops, & Hobart, 2015). The combined analysis of change events, attributed to the most likely disturbance agent (Pickell, Hermosilla, et al., 2014b), together with the change and post-change information, provides a descriptive richness that enables deconstruction of the components of the forest change. These descriptive change metrics allow for an increased ability to quantify, map, and model both land cover change processes and forest recovery through individual reporting on particular agents of disturbance and land cover dynamics.

The capture of change using remotely sensed data and analytical approaches is established and increasingly considered as operational. Knowledge of historic patterns, types, and trends of forest change are required to inform on the sustainability of management practices, allow for the formation of expectations (e.g., amount of wildfire per year and by epoch), as well as the establishment of baseline conditions. Time series metrics that are based upon annual imagery provide a rich source of data and analytical approaches to meet these information needs. Thus, this research builds upon the image compositing and spectral trend analysis approaches presented in (White et al., 2014) and (Hermosilla et al., 2015), to generate a series of change metrics. We demonstrate the generation of change metrics and the use of these metrics in an object-based change typing approach to attribute both stand replacing and non-stand-replacing changes over a large jurisdictional unit. In so doing, we communicate the nature and performance of various change metrics in the attribution of change type. More broadly, using Landsat TM and ETM+ data representing 1984 to 2012, we demonstrate a capacity for depiction of forest changes on an annual basis. A systematic accuracy assessment protocol for the change year and types is also presented.

2. Study area and data

The study area for this research is the western Canadian province of Saskatchewan, which has an area of 651,900 km^2 (Fig. 1). While the southern area of the province is largely represented by the Canadian Prairies, which are dominated by extensive agriculture, wetlands, and grasslands, the northern portion of the province is comprised of three forested ecozones (Boreal Plains, Boreal Shield, and Taiga Shield) (Rowe, 1996) that account for 58% of the provincial area. Areas of the northern forested ecozones are primarily composed of black spruce (*Picea mariana*) and jack pine (*Pinus banksiana*) and are dominated by large wildfires. These areas are generally considered unmanaged, meaning that there are neither tenure arrangements for forest harvesting nor any fire suppression activities; as such, forest inventory information for these areas is scarce (Brandt et al., 2013). By contrast, more southern latitudes of the forested area are dominated by aspen (*Populus tremuloides*), white spruce (*Picea glauca*), and tamarack (*Larix laricina*), and are subject to sustainable forest management (including fire suppression) with ongoing tenure arrangements allowing for harvest. Forest inventory information is available in some of these areas. Additionally, although fire suppression is more common in managed forests, wildfires still occur annually.

The province of Saskatchewan is covered by 71 scenes (path/rows) of the Landsat Worldwide Referencing System (WRS-2). All available images with less than 70% cloud cover from the United States Geological Survey archive of Level-1-Terrain-Corrected (L1T) Landsat Thematic Mapper (TM) and Landsat Enhanced Thematic Mapper Plus (ETM+) acquired from August 1st ± 30 days from 1984 to 2012 with a total of 7748 candidate images for inclusion in annual best available pixel composites (Table 1). August 1st was selected as the central target acquisition date due to a general correspondence with the growing season for the majority of Canada's terrestrial area (McKenney, Pedlar, Papadopol, & Hutchinson, 2006). As the focus of this work is on forested areas, agricultural lands were identified and excluded from our analyses using a mask provided by Agriculture and Agri-Foods Canada (2011 data; ftp://ftp.agr.gc.ca/pub/outgoing/aesb-eos-gg/Crop_Inventory/).

3. Methodology

An overview of the change detection, characterization, and attribution process is described below and includes: (i) initial image preprocessing and compositing, (ii) detection of changes based on spectral trend analysis, (iii) characterization of change events based on their temporal, geometrical, and spectral metrics, and finally (iv) change attribution to the most likely disturbance agent.

3.1. Pre-processing and image compositing

Initially, the digital numbers of the six optical bands of all Landsat images are converted to surface reflectance values by applying atmospheric correction of the Landsat Ecosystem Disturbance Adaptive Processing System (LEDAPS) algorithm (Masek et al., 2006; Schmidt, Jenkerson, Masek, Vermote, & Gao, 2013). Clouds, and their shadows, are detected and masked using the Fmask algorithm (Zhu & Woodcock, 2012). Fmask is also used to define a water mask, which enable to exclude water bodies from further analysis (Lunetta, Johnson, Lyon, & Crotwell, 2004). Annual best available pixel (BAP) image composites are then created using the pixel-scoring functions described in detail in (White et al., 2014). These functions score each pixel observation for (i) sensor, (ii) acquisition day of year, (iii) distance to clouds and cloud shadows, and (iv) atmospheric opacity. The surface reflectance value of pixel with the highest summation of the four scores is then used in the BAP image composites for a given year, and those pixels without suitable observations are labeled as “no data” and are addressed later in the compositing process.

3.2. Spectral trend analysis based change detection

Changes are detected using the Landsat time series spectral trend analysis protocol presented in (Hermosilla et al., 2015). In addition to detecting and describing changes and trends, this protocol enables the production of annual gap-free surface reflectance composites. The protocol is comprised of four main steps: noise detection, breakpoint detection, contextual analysis, and generation of gap-free composites and is informed by values present for a given pixel

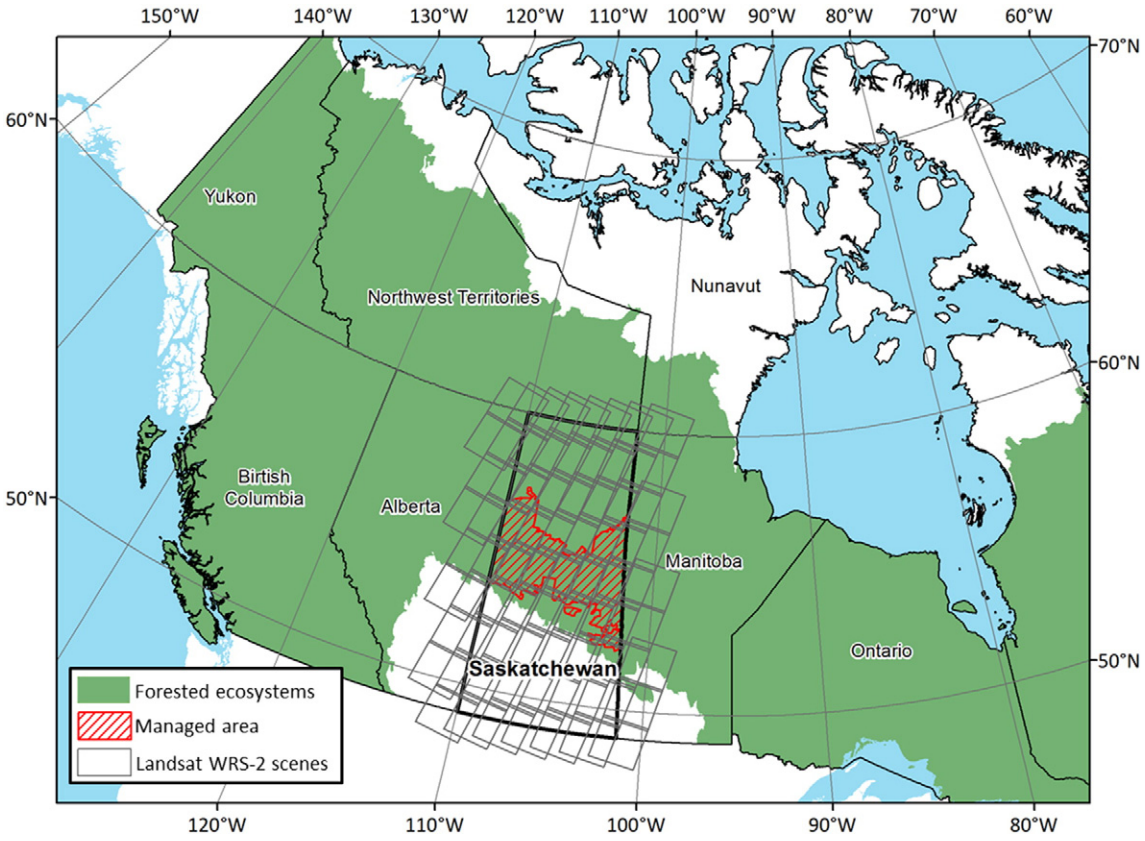

Fig. 1. Study area, Canadian province of Saskatchewan, including the extent of the forested ecosystems within Canada, and the provincial forest management area. Footprints of the 71 Landsat WRS-2 scenes considered are also shown.

Table 1
Number of candidate images available from the United States Geological Survey Landsat archive.

Year	Number of images
1984	172
1985	154
1986	175
1987	169
1988	205
1989	206
1990	174
1991	201
1992	185
1993	176
1994	195
1995	162
1996	196
1997	187
1998	217
1999	381
2000	245
2001	433
2002	366
2003	358
2004	355
2005	344
2006	384
2007	388
2008	381
2009	353
2010	371
2011	416
2012	199
Total	7748

series overtime. A pixel series is the temporal vector of spectral values found for a given pixel.

Initially, a noise detection method is applied to filter anomalous spectral observations resulting from unscreened cloud or cloud shadows, or by haze or smoke, which may be confused with actual change events. The values at a given time are examined in relation to their previous and subsequent spectral values for each Landsat spectral band (Kennedy et al., 2010; Zhu & Woodcock, 2014). If a pixel is detected as an outlier in three or more of the spectral bands they are flagged as noise and removed from the analysis (i.e. labeled as "no data").

Change events in the trajectory of a pixel value through time are detected using a bottom-up breakpoint detection algorithm (Keogh, Chu, Hart, & Pazzani, 2001) using Normalized Burn Ratio (NBR) values (Key & Benson, 2006). First the pixel series composed by n values are divided into $n-1$ segments. The cost of merging each pair of adjacent segments is computed using the Root-Mean-Square Error (RMSE), and the pair with the lowest cost is merged. The cost value is then recomputed for the new segments and the process is iterated until satisfying a stopping criteria. Two stopping criteria are defined: the maximum number of segments and the maximum merging cost allowed, the latter being dynamically adapted during the iteration process to enforce the algorithm to meet the maximum number of segments criteria.

To improve the consistency and the spatial cohesion of the changes—which are detected in the temporal domain—a contextual analysis is then applied in the spatial domain (as detailed in (Hermosilla et al., 2015)). We rank the reliability of correctly predicting the year of a change event, which is inversely related to the number of years of missing data (i.e. pixels labeled as "no data") before, during and after the change event. While detected changes with no or few missing data are considered reliable and labeled with their date of occurrence, changes with missing observations before, during and after the change event are

considered to have a lower reliability. Low-reliability changes that are spatially-adjacent to an observation determined to be of high-reliability within ± one year are re-labeled with the year of occurrence of the more reliable change.

The final step of the integrated protocol is the infilling with proxy values to the pixels labeled as "no data", which is done using the temporal segments produced in the breakpoint detection process to guide a piecewise linear interpolation. This results in gap-free surface reflectance image composites.

3.3. Change characterization

Spectral trend analysis can provide a comprehensive set of descriptors for characterizing change events. The change characterization process enables the depiction of a broad range of change types and conditions, and provides opportunities to build a forest change hierarchy based on the events' properties. In this study, changes are analyzed using object-based image analysis approach (Blaschke, 2010; Ruiz, Recio, Fernandez-Sarria, & Hermosilla, 2011), where change objects are created by the spatial aggregation of changed pixels with same date of occurrence and duration of event, resulting in a total of 1,170,000 change objects for the study area. Change objects are characterized using a comprehensive set of metrics that inform the temporal, spectral and geometric properties of the change events (Table 2).

A set of metrics is derived from the trend analysis to characterize the change events as well as pre- and post-change conditions, which can then be used to attribute the change events. Duration represents the time over which the event takes place. Magnitude variation is the difference between the average spectral values before and after the change event. Pre-change and post-change conditions are characterized by the magnitude variation, duration, and evolution rate (i.e. ratio between magnitude variation and duration) (Hermosilla et al., 2015). Pre- and post-change event trend descriptors are used to provide additional information, but are not used as variables in the attribution model. Additionally, a set of spectral metrics are computed for selected bands and indices: average of the spectral values of the objects before the change event, average and standard deviation after the change event, and range, average and standard deviation of the values of the pixel series for the spectral bands 3, 4, 5, and 7, and for the indices NBR, and Brightness, Greenness and Wetness components from the Tasseled Cap (Crist, 1985; Healey, Cohen, Zhiqiang, & Krankina, 2005). The geometry and shape complexity of the objects is described using area, perimeter, compactness (Bogaert, Rousseau, Van Hecke, & Impens, 2000), shape index (McGarigal & Marks, 1995), and fractal dimension (Krummel, Gardner, & Sugihara, 1987).

Table 2
Summary of the times series change metrics.

Geometrical metrics	
Area	
Perimeter	
Compactness	
Shape index	
Fractal dimension	
Trend analysis metrics	
Duration	
Average change magnitude variation	b4, b5, b7, NBR, TCG, TCW, TCB
Pre-change magnitude variation	NBR
Pre-change duration	
Pre-change evolution rate	NBR
Post-change magnitude variation	NBR
Post-change duration	
Post-change evolution rate	NBR
Spectral metrics	
Average spectral value pre-change	b4, b5, b7, NBR, TCG, TCW, TCB
Average spectral value post-change	b4, b5, b7, NBR, TCG, TCW, TCB
Standard deviation value post-change	b4, b5, b7, NBR, TCG, TCW, TCB
Average pixel series value	b4, b5, b7, NBR, TCG, TCW, TCB
Standard deviation of pixel series values	b4, b5, b7, NBR, TCG, TCW, TCB
Range of pixel series values	b4, b5, b7, NBR, TCG, TCW, TCB

3.4. Change attribution

We propose a hierarchical framework for labeling detected changes (see Fig. 2). This hierarchical approach allows for the characterization and nesting of analogous levels of change based on key criteria, such as duration, spatial extent, rate, or severity (Coops, Wulder, & White, 2006; Kurz, 2010). Using this approach, analogous changes can be placed at the same level, thereby allowing for stratification and nesting of changes. At the highest level, events may be characterized as either change or no change. For changed pixels, time series metrics can inform on the magnitude, duration, and direction of the change. Of these changed pixels, some will be stand replacing (e.g., harvest, wildfire) and others not, with magnitude a key metric for making this distinction. Subtle, non-stand-replacing disturbances, such as changes related to annual variations in vegetation moisture condition can be captured to support scientific investigations (e.g., with stress as a precursor to insect infestations) or related to habitat alterations.

Based on the attribution hierarchy presented in Fig. 2, an unlimited number of change types may theoretically be determined and characterized; however, in this study we focus on four change types that are relevant for reporting and monitoring requirements (White et al., 2014) and those that dominate Saskatchewan's forested ecosystems. Initially, based on the magnitude of a given change event, we differentiate between a range of stand-replacing and non-stand-replacing change types. Within the stand-replacing change types, we establish two categories based on change persistence: long-term and short-term change. Long-term changes in this area principally comprise *Roads*, whereby vegetation is removed for the construction of roads, highways, and access corridors. The linear nature of these features allows them to be distinguished from other long-term change types such as industrial developments or urbanization. Short-term change events comprise either *Fire*, which results in stand mortality, or *Harvest*, which is the temporary removal of trees for utilization. *Non-stand-replacing change* types are characterized as low magnitude, punctual, trend anomalies that relate year-on-year ephemeral changes and that do not lead to a change in land cover class (i.e., phenology, insects, water stress). Changes in this class are related to temporary variations in the vegetation condition. While other classes such as industrial or urban developments are present in our study area, they are rare and will be identified as *Unclassified* in our approach. Herein we focus our efforts on attributing those changes within the study area that occupy the bulk of the change area and that address our information needs, rather than focusing on the characterization of exceptions. Our approach is sufficiently flexible such that objects that remain unclassified can be further characterized and attributed should information needs merit further effort.

Change objects are attributed to one of the four change types using the Random Forest classifier (Breiman, 2001), which develops multiple decision trees (500 in this implementation) based on a random subset of the training samples (collected as defined in Section 3.5.2), where each decision tree division is based on a random subset of the descriptive metrics. Due to the high number of metrics (55) multicollinearity among the descriptive metrics may occur, negatively impacting any attribution model and hence the classification results (Brosofske, Froese, Falkowski, & Banskota, 2014). As a result, we tested for multicollinearity between metrics, and removed metrics with a Pearson's $R > 0.70$. Objects are attributed with the most voted class predicted by each individual tree (Lawrence, Wood, & Sheley, 2006; Pal, 2005). In addition to the class attribution, the Random Forest classifier evaluates the importance of the metrics to predict the classes using the classification mean decrease in value (variable importance measure). This value indicates how much poorer the predictive model would perform without including a particular metric, so a large decrease in accuracy would be expected for highly predictive metric (Louppe & Wehenkel, 2013).

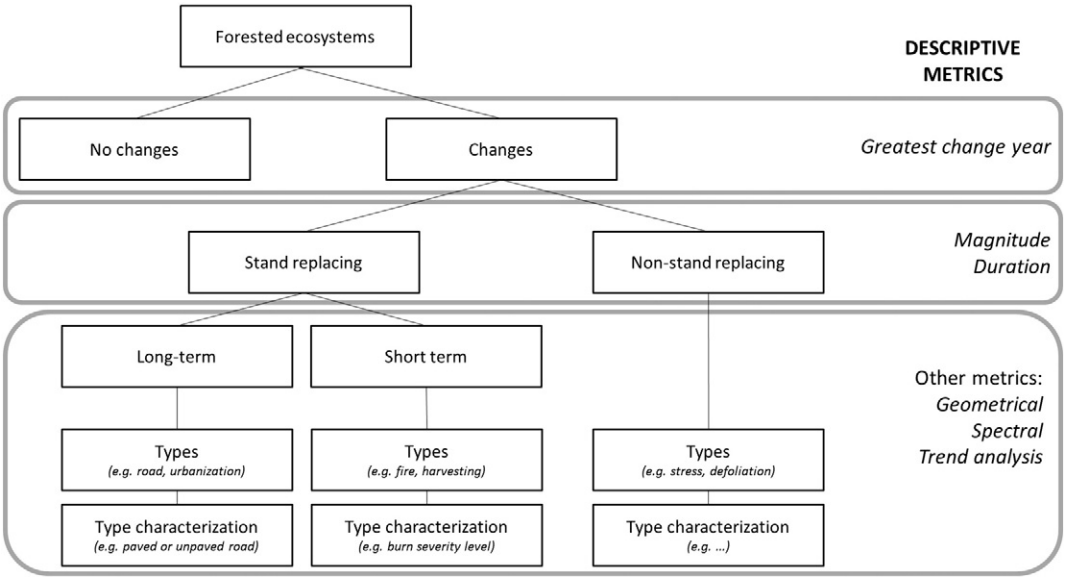

Fig. 2. Land cover change hierarchy scheme (left) and descriptive metrics characterizing each of the levels (right).

The number of votes received by each change class is also used to enrich the attribution results by computing the distance to second voted class as an indicator of attribution confidence (Mitchell, Remmel, Csillag, & Wulder, 2008). This confidence indicator is computed as the ratio (v_2/v_1) between the proportion of votes of the second most voted class (v_2) and the proportion of votes of the assigned class (v_1), and the values rage between 0 (high confidence attributions) and 1 (low confidence attributions). Using this attribution confidence indicator, we avoid attributing a change object to a class when the confidence is low. Instead these change-event objects are unattributed and will require further investigation. We defined as low confidence attributions (and hence labeled as *Unclassified*) objects attributed with a ratio value higher than 0.4. This value was determined using a sensitivity analysis to minimize commission and omission errors, thereby limiting the number of unclassified events. According to our context and information needs, it is preferred to carry an *Unclassified* class than to have low confidence or poor quality attributions.

3.5. Sampling and accuracy assessment

3.5.1. Change detection

A stratified random sampling strategy was used to select validation sites for the change detection (Olofsson et al., 2014) with a minimum number of samples per year in the changed areas (20). In total 1046 point samples were manually interpreted by the same trained person using the annual BAP image composites and Google Earth™ high-resolution imagery. These samples were flagged as either *no change* or *change*, and in the case of change, the year of occurrence was also recorded.

The accuracy on the spatial detection of changes is assessed using a confusion matrix, from which overall user's and producer's accuracies per class were computed to assess the commission and omission errors (Congalton, 1991). To avoid the influence of resampling errors on the results, one-pixel window tolerance is defined (Foody, 2002; Verbyla & Hammond, 1995). In addition to the spatial accuracy, the temporal accuracy is evaluated by comparing the date assigned by the trend analysis based change detection with the reference date.

3.5.2. Change attribution

A restricted-randomization scheme (Chatfield, 1991), which comprised a random selection of the objects stratified by area to ensure the size representativeness and a spatially homogeneous distribution was used to verify the attribution of the change event. A total of 686 samples (i.e. change objects) were again examined using photo-interpretation techniques and the event classified into one of four classes (i.e. *Fire*, *Harvesting*, *Non-stand-replacing change*, and *Road*) defined according to the forest change hierarchy (Fig. 2). Table 3 summarizes the number of samples collected for each change class and their area statistics. These samples were used both as training and validation data. We used the Random Forest out-of-bag error estimation technique, which enables an unbiased estimate of the test set error (Breiman, 2001) when the sample represents the spatial distribution of the classes over the study area (Friedl, Brodley, & Strahler, 1999). This technique uses the reserved training samples (representing approximately 37% of samples for each iteration) that are not used in the construction of a particular classification model. The change class assigned to each object by the classifier and its reference class are compared using two confusion matrices measuring the attribution accuracy at the object and area levels.

4. Results

4.1. Change detection assessment

Analysis of the accuracy of the spatial detection of changes is shown in Table 4. The overall accuracy of the change detection is 92.2%.

Table 3
Summary statistics of the area and number of samples per change class.

Change class	N samples	Average area (ha)	Standard deviation area (ha)	Minimum area (ha)	Maximum area (ha)
Fire	180	323.7	633.1	0.6	4471.7
Harvesting	150	97.7	114.8	2.6	795.5
Non-stand-replacing change	224	8.5	26.1	0.6	240.8
Road	124	34.3	45.4	0.8	370.5

Table 4
Confusion matrix of change detection process. The margin of error is computed for a 0.95 level of confidence.

	Reference			
	Change	No change	User's accuracy	Commission error
Change	539	49	91.7%	8.3%
No change	33	425	92.8%	7.2%
Producer's accuracy	94.2%	89.7%		
Omission error	5.8%	10.3%		

Overall accuracy ± margin of error = 92.2% ± 1.6%.

Changes are detected with a commission error (8.3%) higher than the omission error (5.8%), whereas the *no change* category is more affected by omission (10.3%) than commission errors (7.2%). Fig. 3 shows a scatterplot comparing the occurrence date assigned by the change detection method and the reference date for the change samples correctly detected. The majority of the changes (91.1%) are correctly labeled to their observed change date, that is, they are located in the diagonal of Fig. 3. Most of the errors (6.5%) are caused by the detection of the changes one year after their actual occurrence date, while 1.1% of cases are erroneously labeled one year before the actual change. The remaining errors (1.1%) are produced by change pixels detected two or more years after the actual date. Date labeling errors are mostly related to absence of observations in the years of disturbance, and to occurrence of multiple changes in a given location.

4.2. Change characterization

The selection process based on the multicollinearity reduced the number of metrics from 55 to 17, and these are shown in Fig. 4 ranked by the Random Forest variable importance measure. The average change magnitude variation in band 5 was the most relevant metric and excluding it from the attribution would have resulted in an 11% decrease in accuracy, followed by the standard deviation of post-change surface reflectance in band 5 (9.3%), and area (8.7%), each of them from one of the three metric groups defined (i.e. change, spectral, and geometrical metrics). The ranking also indicates the average spectral value pre-change in band 4 (7.4%), average spectral value post-change in NBR (6.4%), average change magnitude variation in band 4 (4.8%), standard deviation value post-change in NBR (4.7%), and the geometrical compactness (4.4%), among the most discriminant descriptive metrics. Fig. 5 illustrates the relationship between the change classes and their metrics. *Fire* exhibits a well-defined spectral response before (Fig. 5.d), during (Fig. 5.a), and after (Fig. 5.e) the change event, and has little spectral confusion with *Harvesting*, especially during (Fig. 5.a) and after the event (Fig. 5.b and Fig. 5.e). Less spectral separability is found for *Road* and *Non-stand-replacing change*. Geometrically, *Fire* has the largest area range whereas *Non-stand-replacing change* events present the smallest extent (Fig. 5.c), and *Road* objects are highly compact (low compactness values) (Fig. 5.f). In contrast, *Non-stand-replacing change* objects are better distinguished by high compactness values, since they represent low-magnitude changes progressing over the time. Low confidence attributions resulted in 19.5% of the change objects being flagged as *Unclassified*, which represents 10.3% of the total area changed.

4.3. Change attribution assessment

The confusion matrix of the change attribution assessment at object-level is shown in Table 5, where the overall accuracy is 91.6%. *Fire* shows the lowest commission (2.2%) and omission (3.2%) errors and good separability with *Harvesting* and *Road* classes. *Road* has the highest commission (13.2%) and omission (20.2%) errors and most of its commission errors are with *Harvesting* and *Non-stand-replacing change*. Table 6 shows the confusion matrix of the change attribution by area. The overall accuracy is 98% and is mainly driven by the large size of *Fire* class objects. Compared to object-level assessment results, errors are reduced for the stand replacing change classes (*Fire* and *Harvesting*) and slightly augmented for *Non-stand-replacing change*. For *Road* omission error is reduced whereas commission error is augmented, both about 6%.

4.4. Change dynamics in Saskatchewan

The annual changed area by change class across the province from 1985 to 2011 is shown in Fig. 6. Overall, fire is markedly the dominant

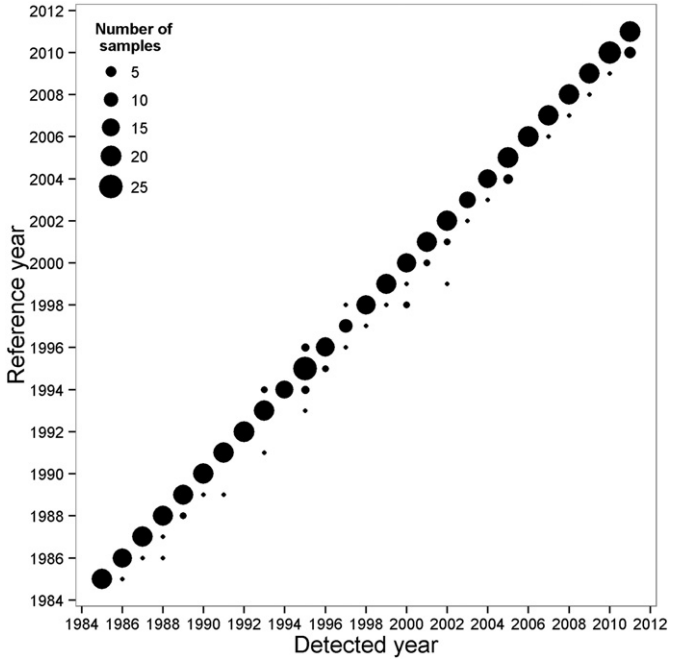

Fig. 3. Scatterplot of detected against reference change year.

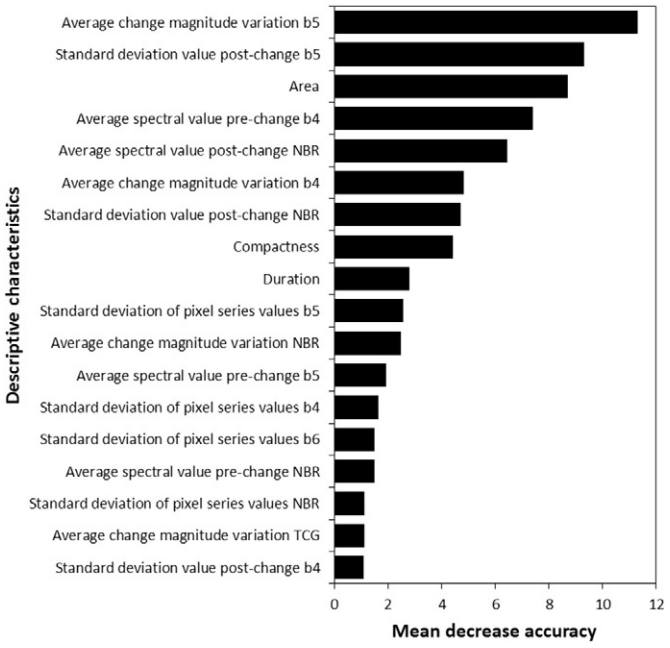

Fig. 4. Descriptive characteristics ranked by their classification mean decrease in accuracy.

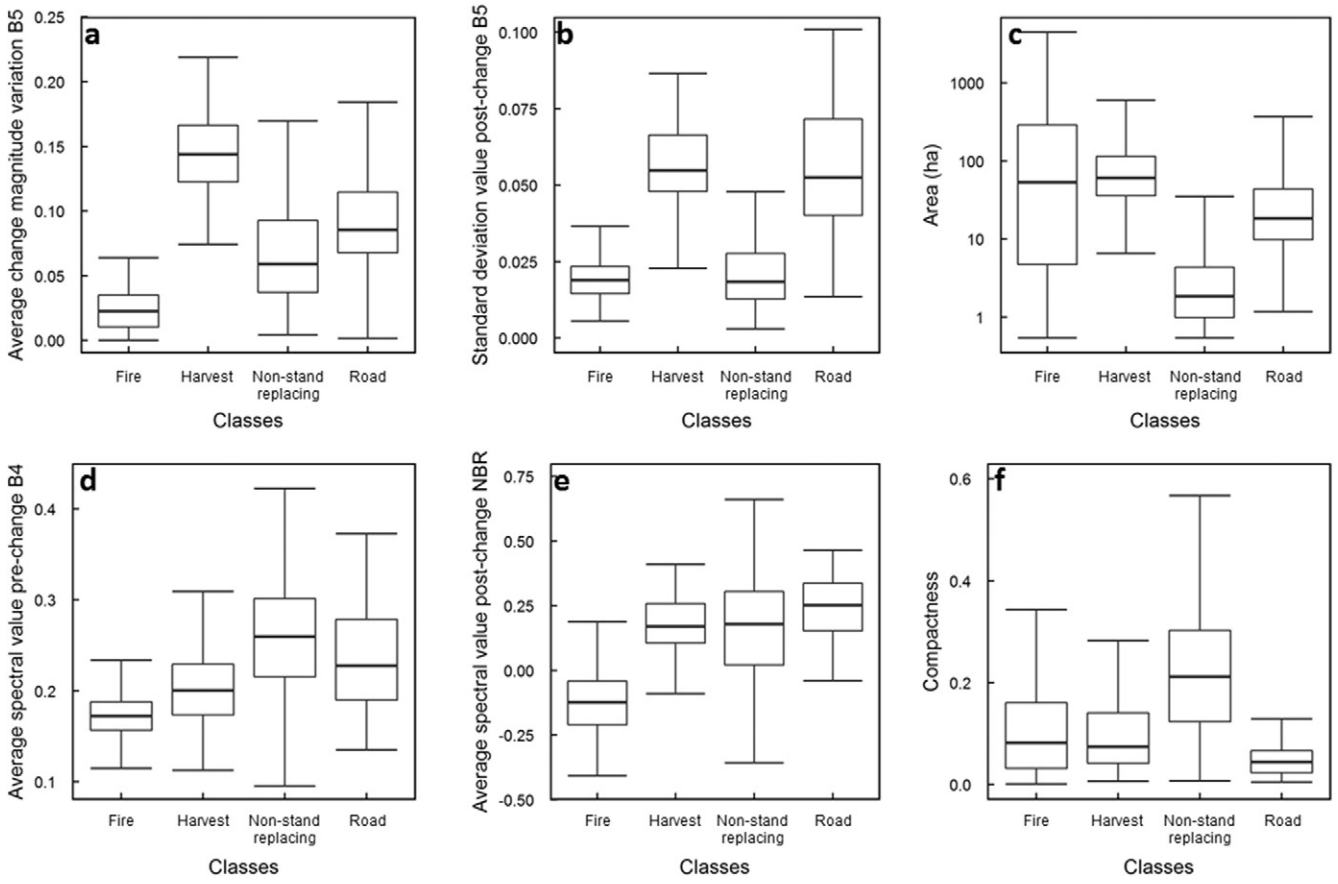

Fig. 5. Relationship between classes and change descriptive characteristics: (a) Average change magnitude variation in band 5, (b) standard deviation value post-change in band 5, (c) area, (d) average spectral value pre-change in band 4, (e) standard deviation value post-change in NBR, and (f) compactness.

stand-replacing change (68.1% of changed areas), followed by harvesting (1.8%), and roads (0.3%). Subtle changes in vegetation condition comprise a notable proportion of the detected changes (19.5%). Over the 30 year period analyzed, fire burnt 344,584 ha ($\sigma = 313{,}543$ ha) annually, with three years showing exceptionally high fire activity (i.e. 1995, 2006, 2010), and two years with notably low fire activity (i.e. 1986, 1997). Harvesting activities were responsible for changes in 9134 ha ($\sigma = 5392$ ha) annually on average, and construction of roads modified an average of 1685 ha ($\sigma = 1630$ ha) annually. The extent affected by non-stand-replacing low-magnitude changes in vegetation condition is 98,676 ha ($\sigma = 80{,}746$ ha) annually, ranging from 2000 ha in 1990 to over 300,000 ha in 2003.

The results reveal that fire is the principal disturbance event in Saskatchewan. However, the annual area burned is extremely variable, linked to annual weather patterns and variations in temperature and precipitation (Delong & Tanner, 1996). Geographically (Fig. 7), northernmost latitudes, which typically have no fire suppression, are prone to large wildfires. In contrast, fire suppression activities are more common in areas with commercial forestry activities and in proximity to populated areas, resulting in smaller wildfire events and less area burnt (Fig. 8.a). Non-stand-replacing changes are more prominent in the forested areas of southern Saskatchewan, and are particularly common in areas dominated by wetlands and grasslands. In these areas, the vegetation changes reflect episodes closely related with hydrological regimes and precipitation, such as vegetation stress or desiccation processes (Lichtenthaler, 1996). The construction of roads (see Fig. 8.c) exhibits variable behavior with two notable peaks in 1998 and 2002, followed by a decreasing trend from 2003 towards. The 1998 peak was dominated by activity within the managed forest zone, with the 2002 peak dominated by road development outside of the managed forest zone. Road developments in the managed forests can be for supporting harvesting or providing general transportation functions, with road developments outside of the managed forest related to new roads, or twinning of existing highway infrastructure. The annual area attributed to harvesting activities (Fig. 8.b) displays similar behavior to the Provincial total actual harvest volume reported

Table 5
Change attribution confusion matrix at object level. The margin of error is computed for a 0.95 level of confidence.

	Reference					
	Fire	*Harvesting*	*Non-stand-replacing change*	*Road*	User's accuracy	Commission error
Fire	174		3	1	97.8%	2.2%
Harvesting		134	2	10	91.8%	8.2%
Non-stand-replacing change	6	6	214	14	89.2%	10.8%
Road		10	5	99	86.8%	13.2%
Producer's accuracy	96.7%	89.3%	95.5%	79.8%		
Omission error	3.3%	10.7%	4.5%	20.2%		

Overall accuracy $\pm$ margin of error $= 91.6\% \pm 2.1\%$.

Table 6
Change attribution confusion matrix at area level. The margin of error is computed for a 0.95 level of confidence.

	Reference					
	Fire	*Harvesting*	*Non-stand-replacing change*	*Road*	User's accuracy	Commission error
Fire	58,245.66		4.05	123.66	99.8%	0.2%
Harvesting		13,835.25	11.97	381.69	97.2%	2.8%
Non-stand-replacing change	17.19	121.59	1710.9	78.12	88.7%	11.3%
Road		701.28	166.14	3672.72	80.9%	19.1%
Producer's accuracy	100.0%	94.4%	90.4%	86.3%		
Omission error	0.0%	5.6%	9.6%	13.7%		

Overall accuracy ± margin of error = 98.0% ± 1.1%.

(Government of Saskatchewan, 2012) and those reported in (Masek et al., 2011). The decline of harvesting and road building activities in the mid-2000s can be linked to a slow-down in the forest industry, as industrial forestry activities are closely related to the economic health of the United States, lumber prices, and various export opportunities (Masek et al., 2011).

5. Discussion

In this paper we apply spectral trend based analysis to 30 years of Landsat TM and ETM+ data over the province of Saskatchewan to detect, characterize, and attribute changes. To do so, we have developed cloud-free seamless annual image composites considering more than 7700 Landsat candidate images from the 71 scenes of the WRS-2 that cover the 651,900 km^2 extent of the study province from 1984 to 2012.

The change detection assessment results indicate that analysis of Landsat's spectral trends provides the capacity to detect both subtle and dramatic changes with high spatial (Table 4) and temporal (Fig. 3) accuracies. Detecting and dating change events with high confidence and reliability is imperative, since the subsequent steps (i.e. characterization and attribution) are built upon the changes detected in this initial stage.

Changes are characterized using a suite of metrics that provide information about different aspects of the change events, such as their geometry and shape, duration and spectral variation, or pre- and post-change spectral dynamics. While results show that some metrics are more relevant to distinguish among the change categories considered (Fig. 4 and Fig. 5), other metrics may complement the attribution results with additional information about the particular behavior of changes, and also post- and pre-disturbance scenarios. The specific contribution of the descriptive metrics, however, will likely vary when used to describe other landscapes containing additional agents of disturbance.

The characterization of the changes provided by the descriptive metrics enables us to accurately attribute change events to their agent of disturbance. The stand-replacing fire and harvesting events are successfully distinguished; however the results show that harvest events are often confused with roads, as harvesting objects are sometimes merged with roads during the delineation process due to their close proximity and spectral similarity (i.e., consider a road within a cut block). Roads themselves are not a uniform feature, ranging from narrow gravel industrial roads with encroaching vegetation through to wide paved highways with medians and roadside ditches. Indeed, due to the spatial resolution of Landsat TM and ETM+ data, roads are often sub-pixel and can thus appear fragmented or are mixed with other change types (Stewart, Wulder, McDermid, & Nelson, 2009). As a result, roads are difficult to attribute accurately.

The accuracies found for the metric-supported change attribution enable us to distinguish between agents of disturbance and, hence, to independently report change events in the boreal forest for a given information need (e.g., informing reports on forest management activities

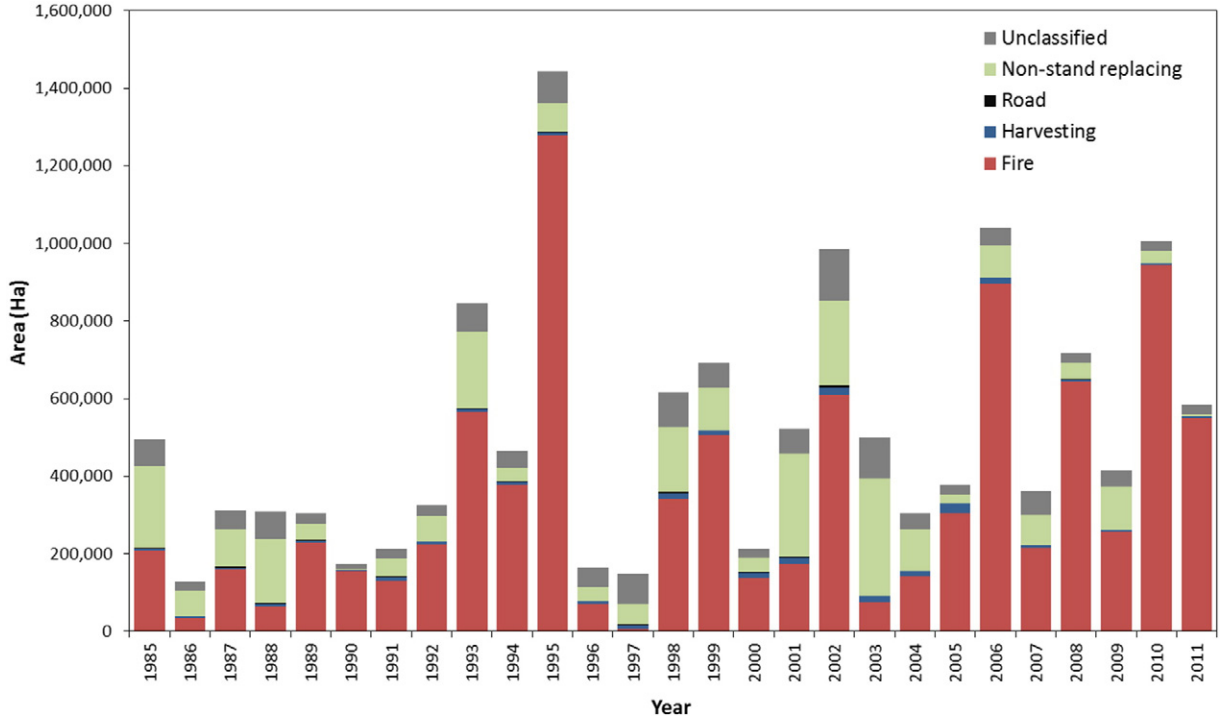

Fig. 6. Total changed area by year and change class.

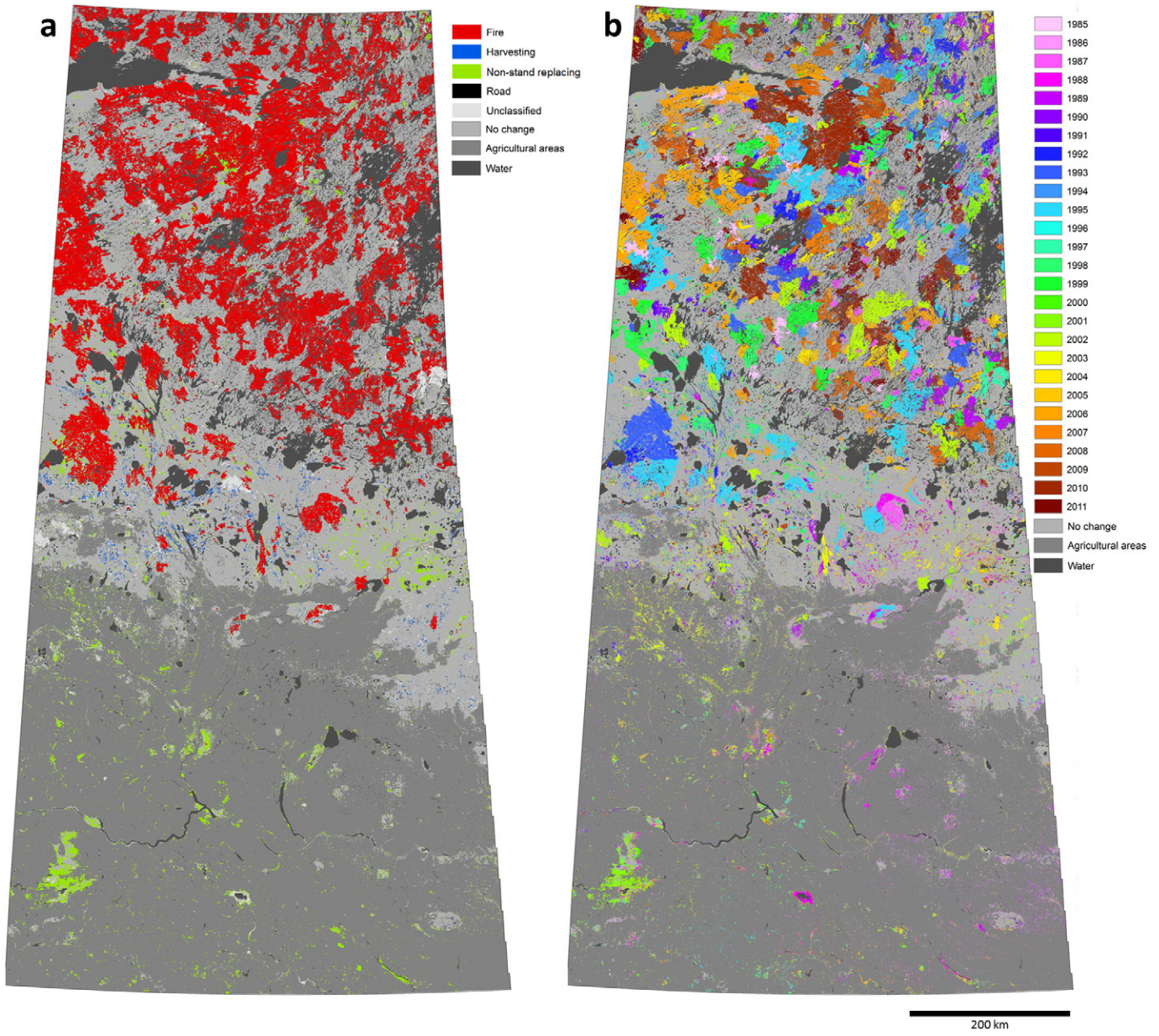

Fig. 7. (a) Distribution of change events attributed to change class; and (b) change events per year.

and documenting and accounting for wildfires). Additionally spectral trend analysis allows for the detection of subtle changes, that is, capturing and distinguishing non-stand- replacing changes, which are commonly unreported. The results presented here, however, raise the possibility of complementing the typically reported stand replacing disturbance rates with increasingly detailed information about the dynamics of subtle vegetation changes across the landscape. Using the information provided by the classifier, we are able to assign an attribution confidence to each change based on the distance between the most likely and second most likely classes (Mitchell et al., 2008). This enables us to flag events with low confidence and to prevent the inclusion of gross errors and rare events (either in space or time) to the attribution results. By doing this, we leave open the possibility of further interrogation and characterization of unclassified change objects based on pre- and post-change descriptors and/or additional metrics. Our study is focused in the province of Saskatchewan, but the final aim is to apply this approach across Canada. To extend the attribution from provincial to national, change event categories may require expansion and adaptation to different conditions and regional disturbance regimes across the country.

The analysis of Landsat's spectral trends allows us to partition the forest change hierarchy into several components (see right column in Fig. 2), with the breakpoint analysis of spectral trends enabling detection and dating of major change events (i.e., greatest change year), and allowing us to distinguish between those areas that are undergoing changes versus those that are stable. Once change events are located, metrics such as magnitude variation, duration or post-event spectral response are important to distinguish between stand replacing and non-stand-replacing changes, thus enabling to introduce both a-priori and a-posteriori rules that partition the forest change hierarchy. These descriptive metrics combined with object geometry (e.g. size, shape) and post-change vegetation trends (long-term, short-term changes) allows for typing the change events (e.g. fire, harvesting, road, stress), and also for detailed within-type characterization based on features such as severity, rate, or extent (Coops et al., 2006). Future developments might include additional metrics that enrich the description of

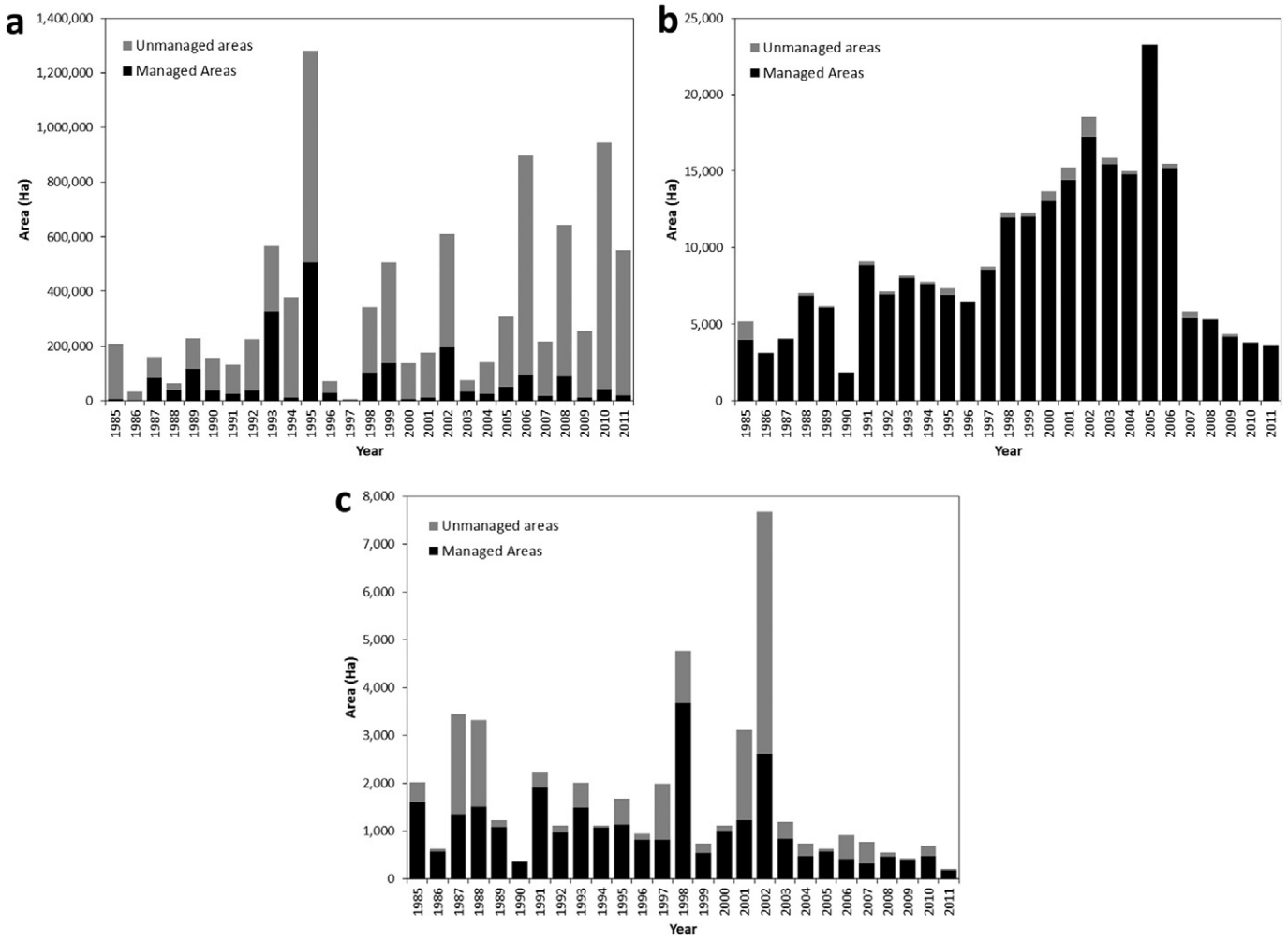

Fig. 8. Detailed annual changed area stratified by managed/unmanaged areas due to (a) fire, (b) harvesting, and (c) road construction (note different ranges on y-axis).

the change events, such as spatial context, and variability of the spectral response within the event.

6. Conclusions

Opening the Landsat archive has greatly increased the use of spectral trend analysis of lengthy data series to explore land cover changes and dynamics. The combination of temporal trend analysis with image compositing techniques enables approaches to be developed and applied over regional or national scales. In this paper, we demonstrate a comprehensive methodology to detect, characterize, and attribute both stand-replacing and subtle changes in forested ecosystems. At the initial level of stratification of change or no change, an overall accuracy of 92.2% (±1.6%, at a 0.95 level of confidence) is found. Similarly, for the change attribution at the object-level, an overall accuracy of 91.6% (±2.1%) is found. When considered by area, overall attribution accuracy is 98.0% (±1.1%). The difference in object level accuracy versus area is largely due to errors found in the labeling of small objects and features such as roads, which have limited spatial extents. The results show accurate temporal and spatial detection of disturbances and change events. These changes are described by temporal, spectral, and geometric (spatial) metrics, which provided a comprehensive description of a range of change characteristics that are used as descriptive variables to attribute change events to agents of disturbance. Fire and harvest show excellent separability, while roads, as expected, are more challenging to discriminate, yet are still captured with >86% user's accuracy. In addition, spectral trend analysis of Landsat data enables non-stand-replacing changes (i.e., changes in vegetation condition) to be detected and distinguished from stand replacing changes. The results of these methods can be used to increase the frequency of mapping and reporting of land cover dynamics, contributing to the improved estimation of change rates in forested ecosystems.

Acknowledgments

This research was undertaken as part of the "National Terrestrial Ecosystem Monitoring System (NTEMS): Timely and detailed national cross-sector monitoring for Canada" project jointly funded by the Canadian Space Agency (CSA) Government Related Initiatives Program (GRIP) and the Canadian Forest Service (CFS) of Natural Resources Canada. We appreciate the time, effort, and insight offered by the journal editors and reviewers.

References

Andrew, M. E., Wulder, M. a., & Coops, N. C. (2012). Identification of de facto protected areas in boreal Canada. *Biological Conservation*, *146*(1), 97–107. http://dx.doi.org/10.1016/j.biocon.2011.11.029.

Banskota, A., Kayastha, N., Falkowski, M. J., Wulder, M. a., Froese, R. E., & White, J. C. (2014). Forest monitoring using Landsat Time Series Data: A review. *Canadian Journal of Remote Sensing*, *40*(March 2015), 362–384. http://dx.doi.org/10.1080/07038992.2014.987376.

Blaschke, T. (2010). Object based image analysis for remote sensing. *ISPRS Journal of Photogrammetry and Remote Sensing*, *65*(1), 2–16. http://dx.doi.org/10.1016/j.isprsjprs.2009.06.004.

Bogaert, J., Rousseau, R., Van Hecke, P., & Impens, I. (2000). Alternative area-perimeter ratios for measurement of 2D shape compactness of habitats. *Applied Mathematics and Computation*, *111*(1), 71–85. http://dx.doi.org/10.1016/S0096-3003(99)00075-2.

Bolton, D. K., Coops, N. C., & Wulder, M. A. (2015). Characterizing residual structure and forest recovery following high-severity fire in the western boreal of Canada using Landsat Time-Series and airborne Lidar data. *Remote Sensing of Environment*, *163*, 48–60.

Brandt, J. P. (2009). The extent of the North American boreal zone. *Environmental Reviews*, *17*, 101–161. http://dx.doi.org/10.1139/A09-004 (NA).

Brandt, J. P., Flannigan, M. D., & Maynard, D. G. (2013). An introduction to Canada's boreal zone: Ecosystem processes, health, sustainability, and environmental issues1. *226*, 207–226 (December). Retrieved from http://www.nrcresearchpress.com/doi/abs/10.1139/er-2013-0040

Breiman, L. (2001). Random forests. *Machine Learning*, *45*(1), 5–32 (Retrieved from http://www.springerlink.com/index/U0P06167N6173512.pdf).

Brosofske, K. D., Froese, R. E., Falkowski, M. J., & Banskota, A. (2014). A review of methods for mapping and prediction of inventory attributes for operational forest management. *Forest Science*, *60*(2)http://dx.doi.org/10.5849/forsci.12-134.

Chatfield, C. (1991). Avoiding statistical pitfalls. *Statistical Science*, *6*(3), 240–268 (Retrieved from http://projecteuclid.org/euclid.ss/1177011686).

Cole, L. E. S., Bhagwat, S. a., & Willis, K. J. (2014). Recovery and resilience of tropical forests after disturbance. *Nature Communications*, *5*, 3906. http://dx.doi.org/10.1038/ncomms4906.

Congalton, R. (1991). A review of assessing the accuracy of classifications of remotely sensed data. *Remote Sensing of Environment*, *46*, 35–46 Retrieved from http://www.sciencedirect.com/science/article/pii/003442579190048B

Coops, N. C., Wulder, M. A., & White, J. C. (2006). Identifying and describing forest disturbance and spatial pattern: Data selection issues and methodological implications. In M. A. Wulder, & S. E. Franklin (Eds.), *Understanding Forest Disturbance and Spatial Pattern (pp. 31–61)*. CRC Press.

Crist, E. (1985). A TM tasseled cap equivalent transformation for reflectance factor data. *Remote Sensing of Environment*, *306*, 301–306.

Delong, S. C., & Tanner, D. (1996). Managing the pattern of forest harvest: Lessons from wildlife. *Biodiversity and Conservation*, *5*.

Foody, G. M. (2002). Status of land cover classification accuracy assessment. *Remote Sensing of Environment*, *80*, 185–201.

Fraser, R., Olthof, I., Carrière, M., Deschamps, A., & Pouliot, D. (2012). Mapping afforestation and deforestation from 1974 to 2012 using Landsat Time-Series stacks in Yulin district, a key region of the Three-North Shelter region, China. *Polar Record*, *48*(01), 83–93. http://dx.doi.org/10.1017/S0032247411000477.

Frazier, R. J., Coops, N. C., Wulder, M. a., & Kennedy, R. (2014). Characterization of aboveground biomass in an unmanaged boreal forest using Landsat temporal segmentation metrics. *ISPRS Journal of Photogrammetry and Remote Sensing*, *92*, 137–146. http://dx.doi.org/10.1016/j.isprsjprs.2014.03.003.

Friedl, M. a., Brodley, C. E., & Strahler, A. H. (1999). Maximizing land cover classification accuracies produced by decision trees at continental to global scales. *IEEE Transactions on Geoscience and Remote Sensing*, *37*(2 II), 969–977. http://dx.doi.org/10.1109/36.752215.

Gómez, C., White, J. C., & Wulder, M. a. (2011). Characterizing the state and processes of change in a dynamic forest environment using hierarchical spatio-temporal segmentation. *Remote Sensing of Environment*, *115*(7), 1665–1679. http://dx.doi.org/10.1016/j.rse.2011.02.025.

Gong, P., & Xu, B. (2003). Remote sensing of forests over time. In remote sensing of forest environments concepts and case studies. pp. 301–333. Retrieved from http://books.google.com/books?hl=en&lr=&id=1JVdXQU9qmYC&pgis=1

Government of Saskatchewan (2012). 2012 Report on Saskatchewan forests. Retrieved from http://www.environment.gov.sk.ca/adx/aspx/adxGetMedia.aspx?DocID=121,104,81,1,Documents&MediaID=dd2b722e-b4fb-491e-9025-b107df7263dc&Filename=2012+Report+on+Saskatchewan+Forests.pdf

Griffiths, P., Linden, S. V., Der Kuemmerle, T., & Hostert, P. (2013). A pixel-based Landsat compositing algorithm for large area land cover mapping. *IEEE Journal of Selected Topics in Applied Earth Observations and Remote Sensing*, *6*(5), 2088–2101.

Hansen, M. C., Egorov, A., Roy, D. P., Potapov, P., Ju, J., Turubanova, S., ... Loveland, T. R. (2011). Continuous fields of land cover for the conterminous United States using Landsat data: First results from the Web-Enabled Landsat Data (WELD) project. *Remote Sensing Letters*, *2*(4), 279–288. http://dx.doi.org/10.1080/01431161.2010.519002.

Hansen, M. C., & Loveland, T. R. (2012). A review of large area monitoring of land cover change using Landsat data. *Remote Sensing of Environment*, *122*, 66–74. http://dx.doi.org/10.1016/j.rse.2011.08.024.

Healey, S. P., Cohen, W. B., Zhiqiang, Y., & Krankina, O. N. (2005). Comparison of Tasseled Cap-Based Landsat data structures for use in forest disturbance detection. *Remote Sensing of Environment*, *97*(3), 301–310. http://dx.doi.org/10.1016/j.rse.2005.05.009.

Hermosilla, T., Wulder, M. A., White, J. C., Coops, N. C., & Hobart, G. W. (2015). An integrated Landsat Time Series protocol for change detection and generation of annual gap-free surface reflectance composites. *Remote Sensing of Environment*, *158*, 220–234. http://dx.doi.org/10.1016/j.rse.2014.11.005.

Huang, C., Goward, S. N., Masek, J. G., Thomas, N., Zhu, Z., & Vogelmann, J. E. (2010). An automated approach for reconstructing recent forest disturbance history using dense Landsat Time Series stacks. *Remote Sensing of Environment*, *114*(1), 183–198. http://dx.doi.org/10.1016/j.rse.2009.08.017.

Kennedy, R. E., Yang, Z., & Cohen, W. B. (2010). Detecting trends in forest disturbance and recovery using yearly Landsat Time Series: 1. LandTrendr — Temporal segmentation algorithms. *Remote Sensing of Environment*, *114*, 2897–2910. http://dx.doi.org/10.1016/j.rse.2010.07.008.

Keogh, E., Chu, S., Hart, D., & Pazzani, M. (2001). An online algorithm for segmenting time series. *Data Mining, 2001. ICDM* (pp. 289–296). http://dx.doi.org/10.1109/ICDM.2001.989531.

Key, C. H., & Benson, N. C. (2006). Landscape assessment (LA): Sampling and analysis methods. *USDA Forest Service Gen. Tech. Rep* RMRS-GTR-164-CD.

Krummel, J., Gardner, R., & Sugihara, G. (1987). Landscape patterns in a disturbed environment. *Oikos*, *48*, 321–324 Retrieved from http://www.jstor.org/stable/3565520

Kurz, W. A. (2010). An ecosystem context for global gross forest cover loss estimates. *Proceedings of the National Academy of Sciences of the United States of America*, *107*(19), 9025–9026. http://dx.doi.org/10.1073/pnas.1004508107.

Lawrence, R. L., Wood, S. D., & Sheley, R. L. (2006). Mapping invasive plants using hyperspectral imagery and Breiman Cutler classifications (Random Forest). *Remote Sensing of Environment*, *100*(3), 356–362. http://dx.doi.org/10.1016/j.rse.2005.10.014.

Lehmann, E. A., Wallace, J. F., Caccetta, P. A., Furby, S. L., & Zdunic, K. (2013). Forest cover trends from time series Landsat data for the Australian continent. *International Journal of Applied Earth Observation and Geoinformation*, *21*, 453–462. http://dx.doi.org/10.1016/j.jag.2012.06.005.

Lichtenthaler, H. K. (1996). Vegetation stress: An introduction to the stress concept in plants. *Plant Physiology*, *148*(1–2), 4–14. http://dx.doi.org/10.1016/S0176-1617(96)80287-2.

Louppe, G., & Wehenkel, L. (2013). Understanding variable importances in forests of randomized trees. *Advances in Neural Information Processing Systems*, *26*, 431–439 Retrieved from http://papers.nips.cc/paper/4928-understanding-variable-importances-in-forests-of-randomized-trees

Lunetta, R. S., Johnson, D. M., Lyon, J. G., & Crotwell, J. (2004). Impacts of imagery temporal frequency on land-cover change detection monitoring. *Remote Sensing of Environment*, *89*(4), 444–454.

Masek, J. G., Cohen, W. B., Leckie, D., Wulder, M. a., Vargas, R., de Jong, B., & Smith, W. B. (2011). Recent rates of forest harvest and conversion in North America. *Journal of Geophysical Research*, *116*(G4), 1–22. http://dx.doi.org/10.1029/2010JG001471.

Masek, J. G., Vermote, E. F., Saleous, N. E., Wolfe, R., Hall, F. G., Huemmrich, K. F., ... Lim, T. K. (2006). A Landsat surface reflectance dataset for North America, 1990–2000. *Geoscience and remote sensing letters, IEEE*, *3*(1), 68–72.

McGarigal, K., & Marks, B. (1995). Spatial pattern analysis program for quantifying landscape structure. *97331*(503) Retrieved from ftp://129.24.124.205/gis/lno/jvc/misc/gis/esc442/fragstats/unix/frag.ps

McKenney, D., Pedlar, J., Papadopol, P., & Hutchinson, M. (2006). The development of 1901–2000 historical monthly climate models for Canada and the United States. *Agricultural and Forest …*, *138*(1–4), 69–81. http://dx.doi.org/10.1016/j.agrformet.2006.03.012.

Mitchell, S. W., Remmel, T. K., Csillag, F., & Wulder, M. a. (2008). Distance to second cluster as a measure of classification confidence. *Remote Sensing of Environment*, *112*, 2615–2626. http://dx.doi.org/10.1016/j.rse.2007.12.006.

Olofsson, P., Foody, G. M., Herold, M., Stehman, S. V., Woodcock, C. E., & Wulder, M. a. (2014). Good practices for estimating area and assessing accuracy of land change. *Remote Sensing of Environment*, *148*, 42–57. http://dx.doi.org/10.1016/j.rse.2014.02.015.

Pal, M. (2005). Random Forest classifier for remote sensing classification. *International Journal of Remote Sensing*, *26*(1), 217–222. http://dx.doi.org/10.1080/01431160412331269698.

Pickell, P. D., Gergel, S. E., Coops, N. C., & Andison, D. W. (2014a). Monitoring forest change in landscapes under-going rapid energy development: Challenges and new perspectives. *Land*, *3*, 617–638. http://dx.doi.org/10.3390/land3030617.

Pickell, P. D., Hermosilla, T., Coops, N. C., Masek, J. G., Franks, S., & Huang, C. (2014b). Monitoring anthropogenic disturbance trends in an industrialized boreal forest with Landsat time series. *Remote Sensing Letters*, *5*(9), 783–792. http://dx.doi.org/10.1080/2150704X.2014.967881.

Powers, R. P., Coops, N. C., Nelson, T., Wulder, M. A., & Drever, C. R. (2013). Integrating accessibility and intactness into large-area conservation planning in the Canadian boreal forest. *Biological Conservation*, *167*, 371–379. http://dx.doi.org/10.1016/j.biocon.2013.08.032.

Rowe, J. S. (1996). Land classification and ecosystem classification. *Environmental Monitoring and Assessment*, *39*(1–3), 11–20. http://dx.doi.org/10.1007/BF00396131.

Roy, D. P., Ju, J., Kline, K., Scaramuzza, P. L., Kovalskyy, V., Hansen, M., ... Zhang, C. (2010). Web-Enabled Landsat Data (WELD): Landsat ETM + composited mosaics of the conterminous United States. *Remote Sensing of Environment*, *114*(1), 35–49. http://dx.doi.org/10.1016/j.rse.2009.08.011.

Ruiz, L. A., Recio, J. A., Fernandez-Sarria, A., & Hermosilla, T. (2011). A feature extraction software tool for agricultural object-based image analysis. *Computers and Electronics in Agriculture*, *76*(2), 284–296. http://dx.doi.org/10.1016/j.compag.2011.02.007.

Schmidt, G. L., Jenkerson, C. B., Masek, J., Vermote, E., & Gao, F. (2013). *Landsat Ecosystem Disturbance Adaptive Processing System (LEDAPS) algorithm description*. (Retrieved from http://pubs.usgs.gov/of/2013/1057/).

Schroeder, T. A., Wulder, M. A., Healey, S. P., & Moisen, G. G. (2011). Mapping wildfire and clearcut harvest disturbances in boreal forests with Landsat time series data. *Remote Sensing of Environment*, *115*(6), 1421–1433. http://dx.doi.org/10.1016/j.rse.2011.01.022.

Stewart, B., Wulder, M., McDermid, G. J., & Nelson, T. A. (2009). Disturbance capture and attribution through the integration of Landsat and IRS-1C imagery. *Canadian Journal of …*, *35*(6), 523–533 (Retrieved from http://www.tandfonline.com/doi/abs/10.5589/m10-006).

Stocks, B. J., Mason, J. a., Todd, J. B., Bosch, E. M., Wotton, B. M., Amiro, B. D., & Skinner, W. R. (2002). Large forest fires in Canada,. *Journal of Geophysical Research*, *108*, 1959–1997. http://dx.doi.org/10.1029/2001JD000484 (August 2002).

Townshend, J. R., Latham, J., Justice, C. O., Janetos, A., Conant, R., Arino, O., ... Tschirley, J. (2011). *Land remote sensing and global environmental change*, *11*, 835–856. http://dx.doi.org/10.1007/978-1-4419-6749-7.

Verbyla, D., & Hammond, T. (1995). Conservative bias in classification accuracy assessment due to pixel-by-pixel comparison of classified images with reference grids. *Remote Sensing*, *16*(3), 581–587 Retrieved from http://www.tandfonline.com/doi/abs/10.1080/01431169508954424

White, J. C., & Wulder, M. A. (2013). The Landsat observation record of Canada: 1972–2012. *Canadian Journal of Remote Sensing*, *39*(6), 455–467 Retrieved from http://www.tandfonline.com/doi/abs/10.1080/01431161.2013.779041

White, J. C., Wulder, M. A., Hobart, G. W., Luther, J. E., Hermosilla, T., Griffiths, P., ... Guindon, L. (2014). Pixel-based image compositing for large-area dense time series applications and science. *Canadian Journal of Remote Sensing*, *40*(3), 192–212. http://dx.doi.org/10.1080/07038992.2014.945827.

Wulder, M. A., Masek, J. G., Cohen, W. B., Loveland, T. R., & Woodcock, C. E. (2012). Opening the archive: How free data has enabled the science and monitoring promise of Landsat. *Remote Sensing of Environment*, *122*, 2–10. http://dx.doi.org/10.1016/j.rse.2012.01.010.

Wulder, M. A., White, J. C., Cranny, M. M., Hall, R. J., Luther, J. E., Beaudoin, A., ... Dechka, J. A. (2008a). Monitoring Canada' s forests. Part 1: Completion of the EOSD land cover project. *Canadian Journal of Remote Sensing*, *34*(6), 549–562.

Wulder, M. A., White, J. C., Goward, S. N., Masek, J. G., Irons, J. R., Herold, M., ... Woodcock, C. E. (2008b). Landsat continuity: Issues and opportunities for land cover monitoring. *Remote Sensing of Environment*, *112*(3), 955–969. http://dx.doi.org/10.1016/j.rse.2007.07.004.

Zhu, Z., & Woodcock, C. E. (2012). Object-based cloud and cloud shadow detection in Landsat imagery. *Remote Sensing of Environment*, *118*, 83–94. http://dx.doi.org/10.1016/j.rse.2011.10.028.

Zhu, Z., & Woodcock, C. E. (2014). Automated cloud, cloud shadow, and snow detection in multitemporal Landsat data: An algorithm designed specifically for monitoring land cover change. *Remote Sensing of Environment*, *152*, 217–234. http://dx.doi.org/10.1016/j.rse.2014.06.012.